

Image Registration and Fusion for Future Formation Flying Systems



Jacqueline Le Moigne

NASA GSFC - Applied Information Sciences Branch

Co-Investigators:

Arlene Cole-Rhodes / Morgan State University

Roger Eastman / Loyola College

Kisha Johnson / Morgan State University

Jeffrey Morisette / GSFC- Lab. for Terrestrial Physics

Nathan Netanyahu / U. of MD and Bar-Ilan U.

Harold Stone / UMBC/GEST Center

Ilya Zavorin / UMBC /GEST Center

Image Registration and Fusion for Future Formation Flying Systems

Goal: Enable on-board or in-situ integration of multiple source data.

Objectives: Develop and evaluate state-of-the-art methodologies for on-board image registration and fusion of multi-sensor data.

Key Innovations:

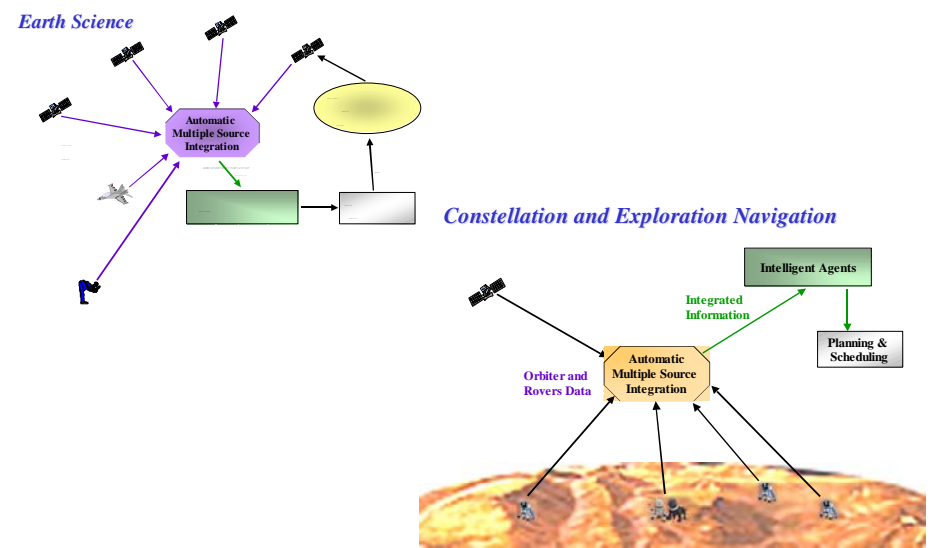
- Development of a framework for independent evaluation of various image registration components
- Use of steerable wavelets for image registration
- Development of a novel wavelet-based dimension reduction technique.

NASA Relevance: Cross Cutting Technologies

- Earth Science: Multi-sensor/multi-mission integration
- Constellation Flying: On-board mission planning
- Exploration: Robot navigation
- Optimizing communication bandwidth and datasets

Accomplishments to date:

- 6 journal and 13 conference publications, including:
- "Earth Science Imagery Registration," IGARSS'03, France, July 2003.
- "Multiresolution Registration of Remote Sensing Imagery by Optimization of Mutual Information Using a Stochastic Gradient," IEEE Trans. on Image Processing, Vol. 12, No. 12, December 2003.



Schedule:

- FY01: Investigate & develop proposed methodologies.
- FY02: Gather test data. Complete methods development.
- FY03: Develop evaluation framework. Comparative studies and validation using Landsat, EOS Core Sites multi-sensor, and Mars data.

Missions/Applications:

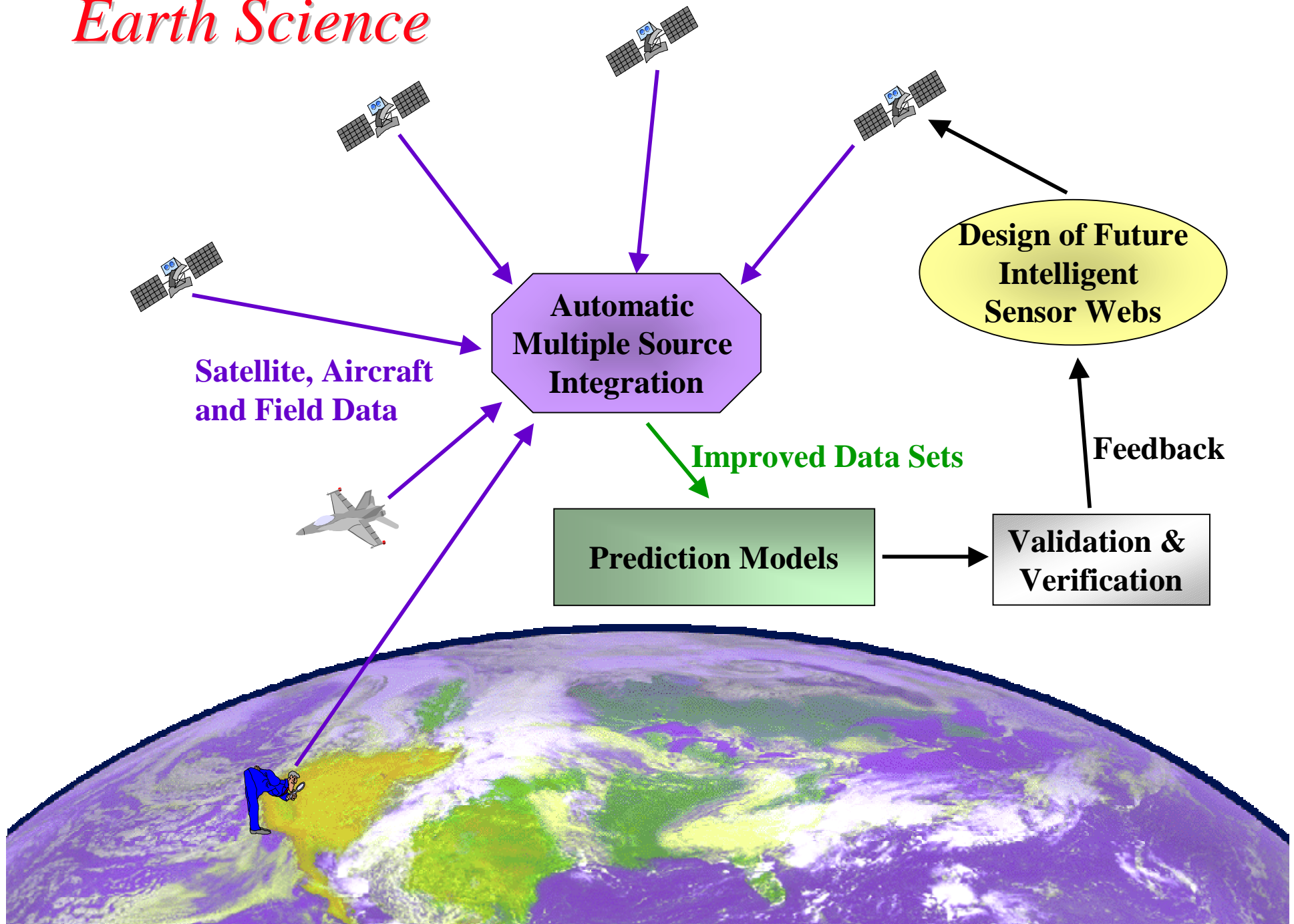
- Landsat Data Continuity Mission (J. Masek, GSFC/923)
- EOS Core Sites (J. Morisette, GSFC/923)
- Invasive Species (J. Schnase, GSFC/923)
- Precipitation Measurement (M. Shepherd, GSFC/910)
- Visualization (G. Shirah, GSFC/930; G. Deardoff, ARC)

Motivations - Applications of Image Registration and Fusion



- Multi-Modal Registration and Fusion
 - New Sensor Calibration, Classification and Unmixing,
 - Extrapolation among Multiple Scales, Temporal, Spatial and Spectral
- Temporal Registration and Fusion
 - Change Detection, Earth/Planet Resources Surveying,
 - Continuity of Data to Build Long-Term Datasets
- Viewpoint Fusion
 - Formation Flying, Planet Exploration, Super-Resolution
- Template/Chip Registration
 - Data Mining, Map Updating
- Scientific Visualization and Virtual Reality

Earth Science



Constellation and Exploration Navigation

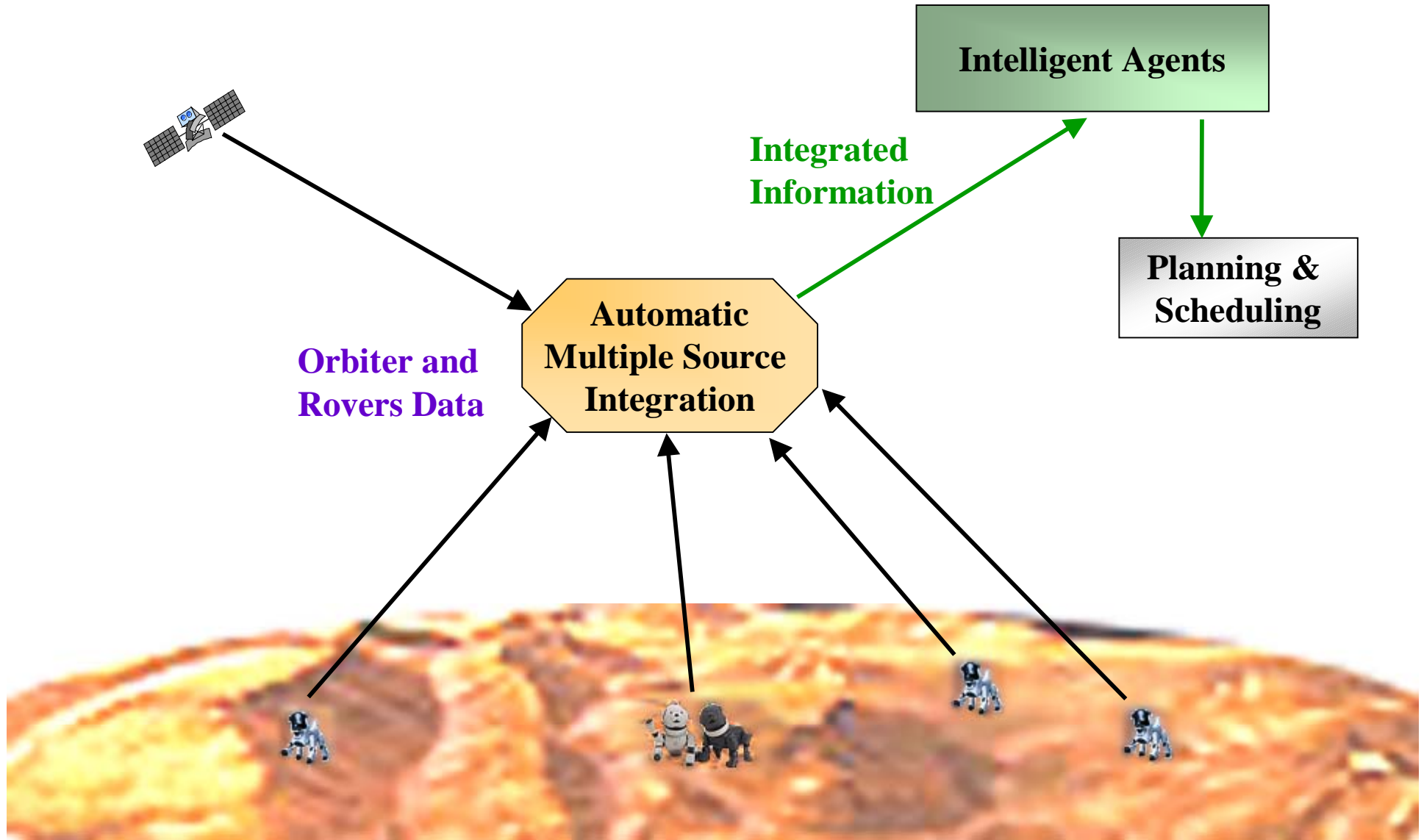




Image Registration Challenges

- Multi-Resolution / Mono- or Multi-Instrument
 - Multi-temporal data
 - Various spatial resolutions
 - Various spectral resolutions
- Sub-Pixel Accuracy
 - 1 pixel misregistration=> 50% error in NDVI computation
- Accuracy Assessment
 - Synthetic data
 - "Ground Truth" (manual registration?)
 - Use down-sampled high-resolution data
 - Consistency ("circular" registrations) studies

Image Registration Components



0 Pre-Processing

- Cloud Detection, Region of Interest Masking, ...

1 Feature Extraction (“Control Points”)

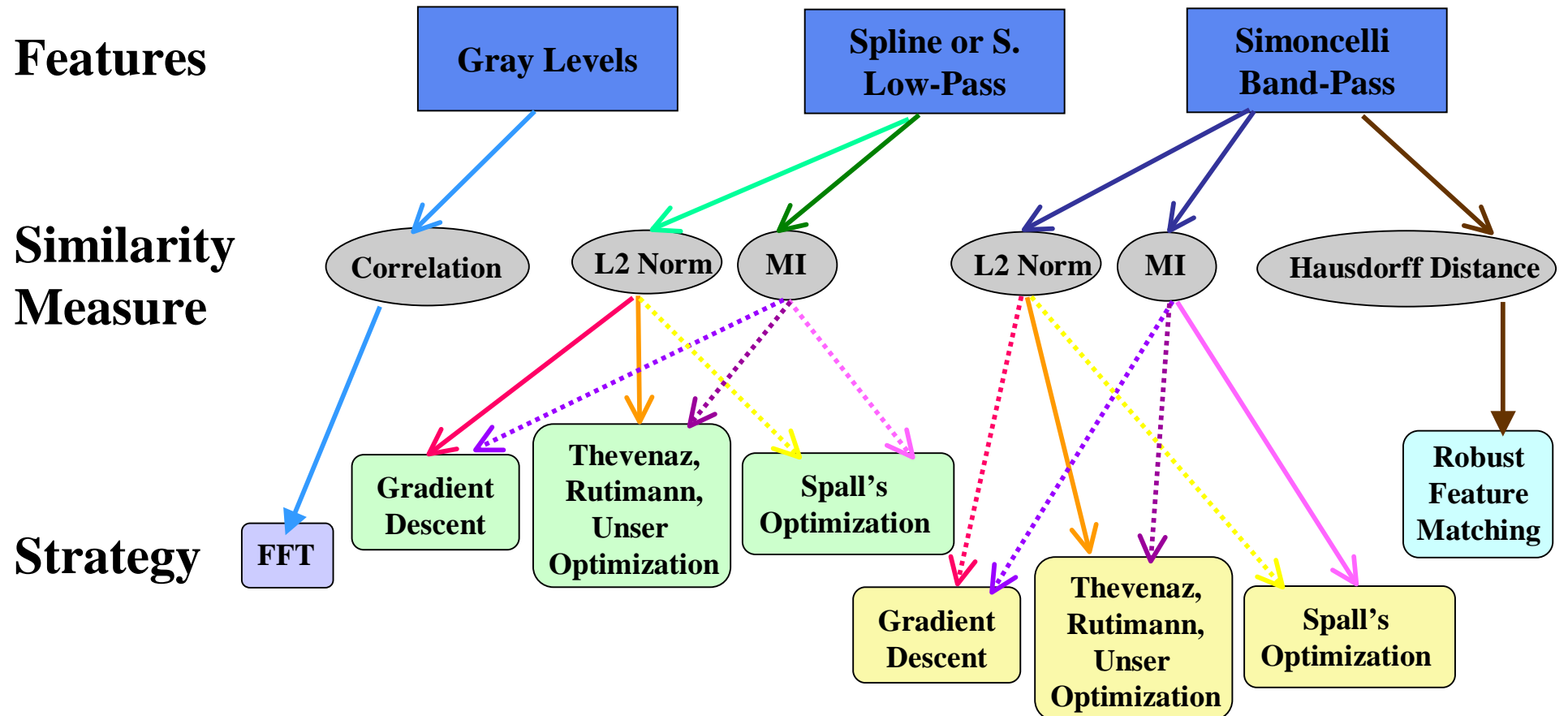
- Edges, Regions, Contours, Wavelet Coefficients, ...

2 Feature Matching

- Spatial Transformation (a-priori knowledge)
- Search Strategy (Global vs Local, Multi-Resolution, ...)
- Choice of Similarity Metrics (Correlation, Optimization Method, Hausdorff Distance, ...)

3 Resampling, Indexing or Fusion

A Framework for the Analysis of Various Image Registration Components



Feature Extraction Experiments



(1) CORRELATION-BASED

a. **Features** = *Gray Levels, Edges or Daubechies Coefficients*

- ==> • Edges/Wavelets More Robust to Noise and Local Intensity Varying
• Phase Correlation Faster
• Wavelet-Based Faster but Edge-Based More Accurate

b. **Features** = *Daubechies and Simoncelli*

- ==> • Daubechies Low-Pass Sub-Band Almost Insensitive to Translation if Features at Least Twice Filters' Sizes
• Simoncelli's More Accurate and Less Sensitive to Noise than Daubechies' Filters
• Translation-Invariant BP Features More robust, less Accurate than LPs

(2) OPTIMIZATION-BASED (L2-BASED GRADIENT LEAST-SQUARES)

Features = *Simoncelli (LP and BP) and Splines*

- ==> * Simoncelli-LP = Best radius of convergence
• Simoncelli-BP = Best for accuracy and consistency
• When CV, Spline features have better accuracy

Mutual Information Experiments



- Correlation vs Mutual Information:
 - Sharper Peak for MI => enables better accuracy
 - MI less sensitive to noise
- MI with Stochastic Gradient
 - Spall's Simultaneous Perturbation Stochastic Approximation (SPSA): based on gradient approximation computed only from measurements of the objective function (200 iterations)
 - On synthetic test data, 0.01 pixel accuracy
 - On Multi-Temporal (cloudy) test data, 0.64 pixel accuracy compared to manual registration
 - On Multi-Sensor test data, 0.34 pixel accuracy

Registration Components

Validation

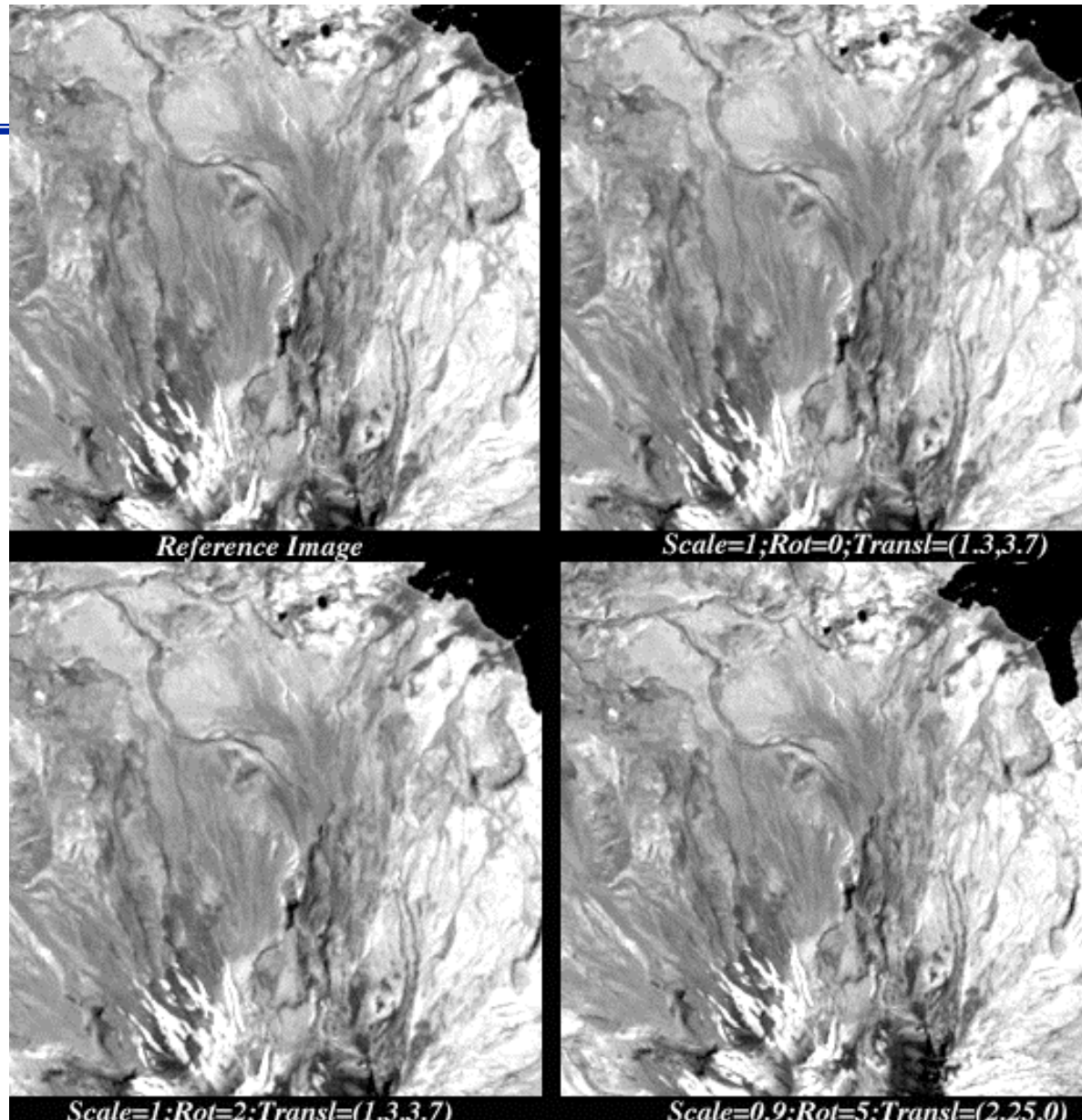


- Controlled Synthetic Test Data
- Meaningful and Representative Data Sets
 - **Multi-Temporal Landsat Data**
 - **Multi-Sensor EOS Validation Core Sites Data**
 - **Mosaic MARS Data**
- Validation Criteria
 - Reliability (Confidence Measurement)
 - Sub-Pixel Accuracy
 - Low Computational Requirements

Test Data Synthetic Images

- Landsat-TM Band 4
 - 512x512 starting scene
 - Extraction of 256x256 Center: **Reference Image**
- Transformation of Starting Scene by:
 - Scales in [0.9,1.1]
 - Translations in [0,4] pixels
 - Rotations in [0,3] degrees
- Extraction of 256x256 centers of transformed scenes: **Input Images**

Synthetic Images



Some Results on Synthetic Test Data

i256_sc0.9						
Scale	0.9014	0.8893	0.9000	0.9000	0.9001	0.9001
Rotation	-0.0392	-0.0056	0.0000	0.0000	0.0005	0.0080
Shift-x	0.0000	0.1376	-0.0002	0.0003	0.0002	-0.0099
Shift-y	-0.0003	0.1059	-0.0005	-0.0013	-0.0022	-0.0251
k_ratio	1.0016	0.9881	1.0000	1.0000	1.0001	1.0001
thetaErr	-0.0392	-0.0056	0.0000	0.0000	0.0005	0.0080
txErr	0.0000	0.1376	-0.0002	0.0003	0.0002	-0.0099
tyErr	-0.0003	0.1059	-0.0005	-0.0013	-0.0022	-0.0251
Global Error	0.0003	0.1747	0.0006	0.0013	0.0022	0.0269
i256_r2_tx1.3_ty3.7						
Scale	1.0001	0.9999	1.0000	1.0000	1.0000	1.0000
Rotation	2.0131	1.9408	2.0002	2.0000	1.9992	2.0004
Shift-x	1.2172	1.1085	1.3001	1.3009	1.2981	1.3049
Shift-y	3.7748	3.6704	3.6997	3.7027	3.6951	3.7052
k_ratio	1.0001	0.9999	1.0000	1.0000	1.0000	1.0000
thetaErr	0.0131	-0.0592	0.0002	0.0000	-0.0009	0.0004
txErr	-0.1313	0.0297	-0.0008	0.0000	0.0013	0.0035
tyErr	0.0918	-0.0998	0.0000	0.0028	-0.0060	0.0057
Global Error	0.1602	0.1041	0.0008	0.0029	0.0061	0.0067
i256_sc0.9_r5_tx2.25						
Scale	0.9018	0.8897	0.9000	0.8999	0.9616	0.9000
Rotation	4.9566	5.0015	4.9996	4.9991	3.8120	5.0080
Shift-x	2.2876	2.018	2.2505	2.2513	-4.3352	2.2517
Shift-y	0.3609	0.3027	-0.0014	-0.0026	4.7762	0.0034
k_ratio	1.0020	0.9885	1.0000	0.9999	1.0685	0.9999
thetaErr	-0.034	0.0016	-0.0004	-0.0009	-1.1880	0.0080
txErr	0.15	0.2777	0.0005	0.0015	-5.2331	0.0019
tyErr	0.2631	0.3732	-0.0024	-0.0047	2.5461	0.0214
Global Error	0.2652	0.4679	0.0024	0.0049	5.6300	0.0215
i256_sc1.1_r3_tx3.1_r2.75						
Scale	1.1002	1.0890	1.1000	1.1000	1.0632	1.1000
Rotation	2.9922	2.8758	3.0001	3.0002	-3.0035	2.9981
Shift-x	2.7988	2.5993	3.1000	3.1002	-3.2838	3.0782
Shift-y	2.6428	2.6139	2.7500	2.7503	-8.8802	2.7507
k_ratio	1.0002	0.9900	1.0000	1.0000	0.9665	1.0000
thetaErr	-0.0078	-0.1242	0.0000	0.0002	-6.0035	-0.0019
txErr	-0.2802	-0.1089	-0.0002	-0.0003	-6.8974	-0.0166
tyErr	-0.1318	-0.4679	0.0001	0.0009	-10.6076	-0.0052
Global Error	0.3096	0.4828	0.0002	0.0010	12.8701	0.0174
MEAN ERROR	0.1569	0.2401	0.0590	0.0019	2.6456	0.0190

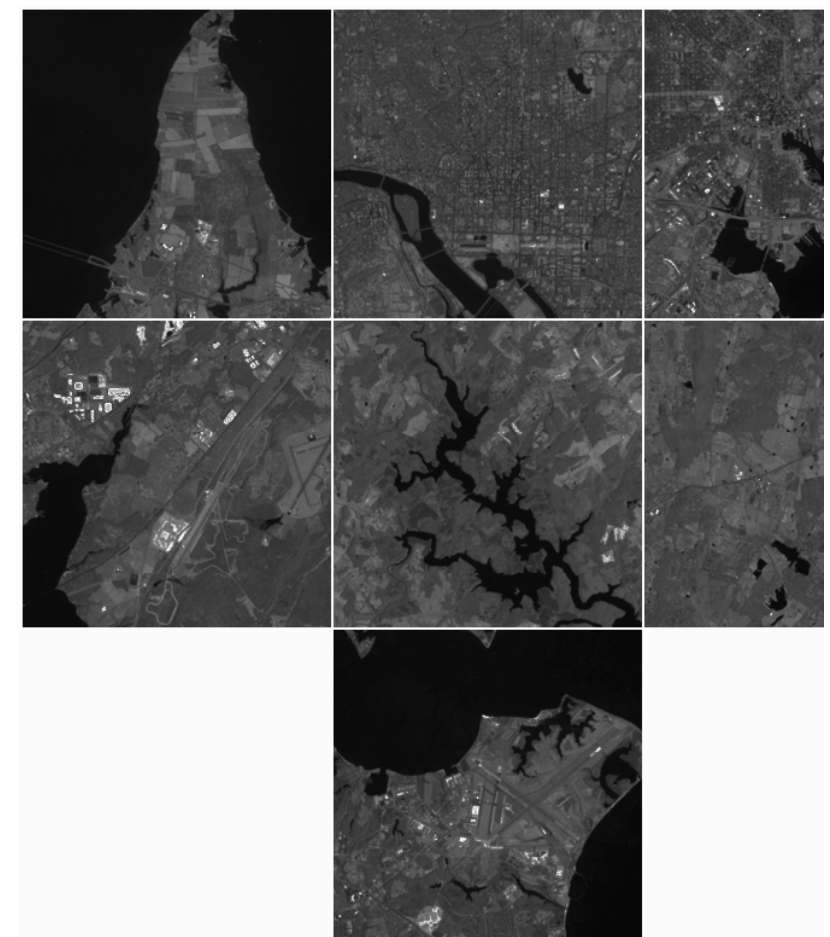
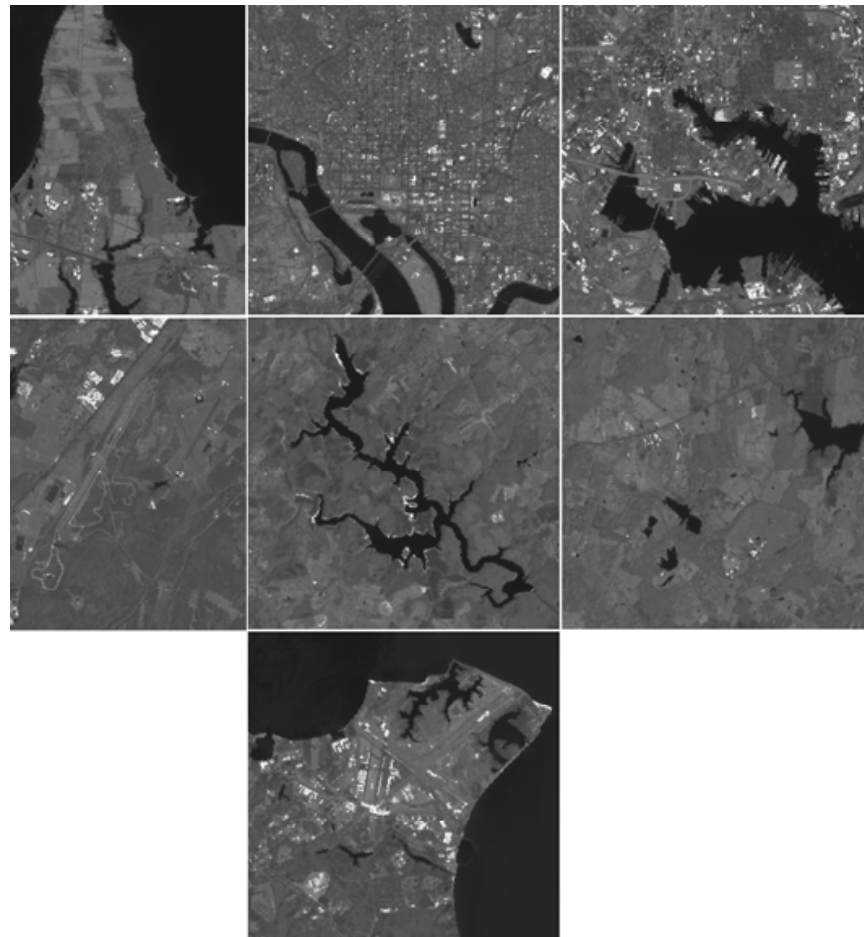
→ Best Accuracy of 0.09 Pixels

Multi-Temporal Landsat Image Registration



- Collaboration: Jeff Masek (GSFC/923): Landsat Data Continuity Mission
- Landsat-5 and -7 Multi-Temporal Data
- 2 Areas, Central VA and DC/Baltimore
- For each area:
 - 1 reference scene with 6 to 8 reference chips (256x256)
 - 4 input scenes, for each:
 - Extract windows corresponding to chips
 - Local registrations chip/window pairs, using Simoncelli-Band Pass Features and Robust Feature Matching
 - Global registration using a generalized LMS
- Accuracies Between 0.21 and 0.59 pixel

Chip-Window Pairs



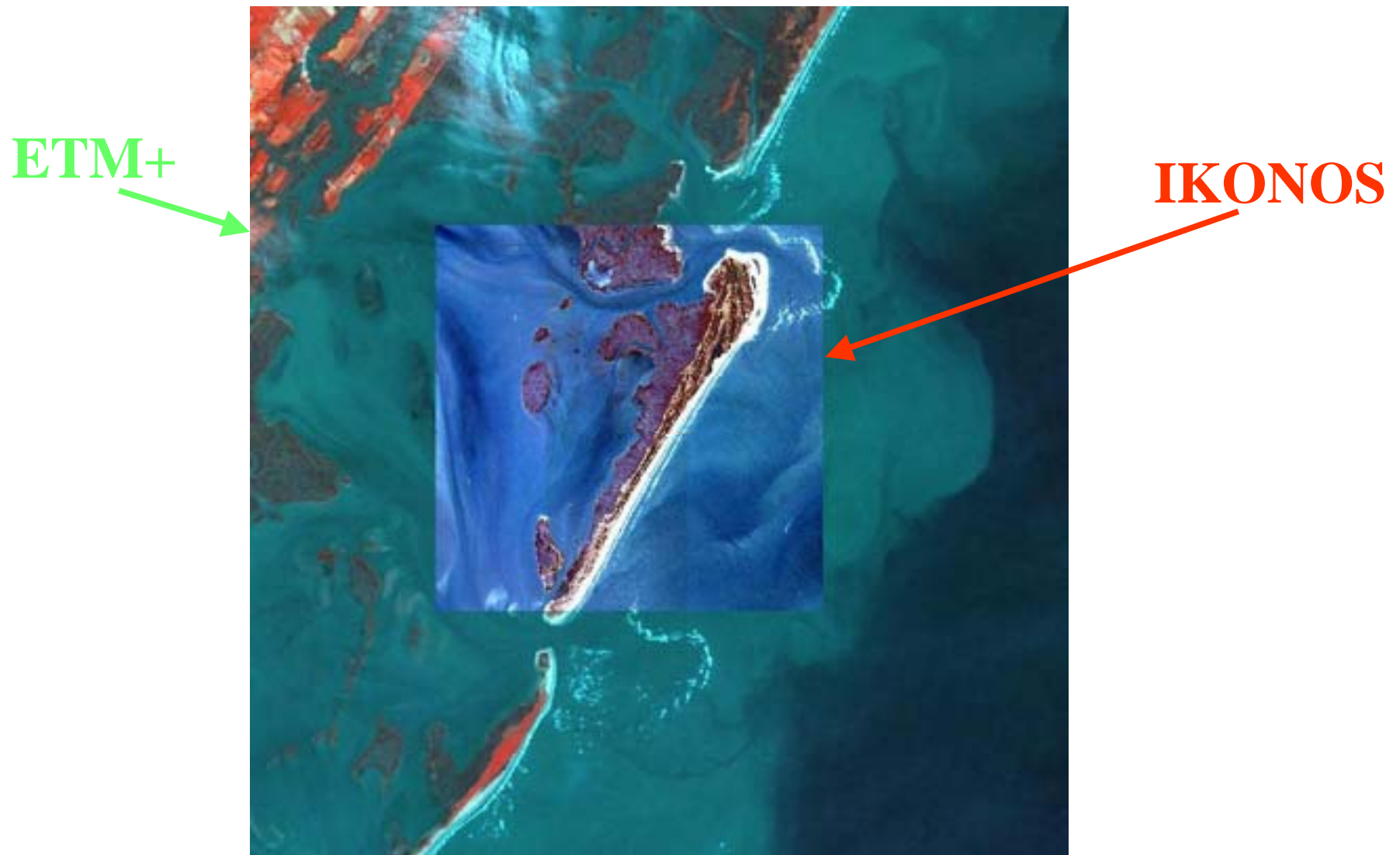
Test Data



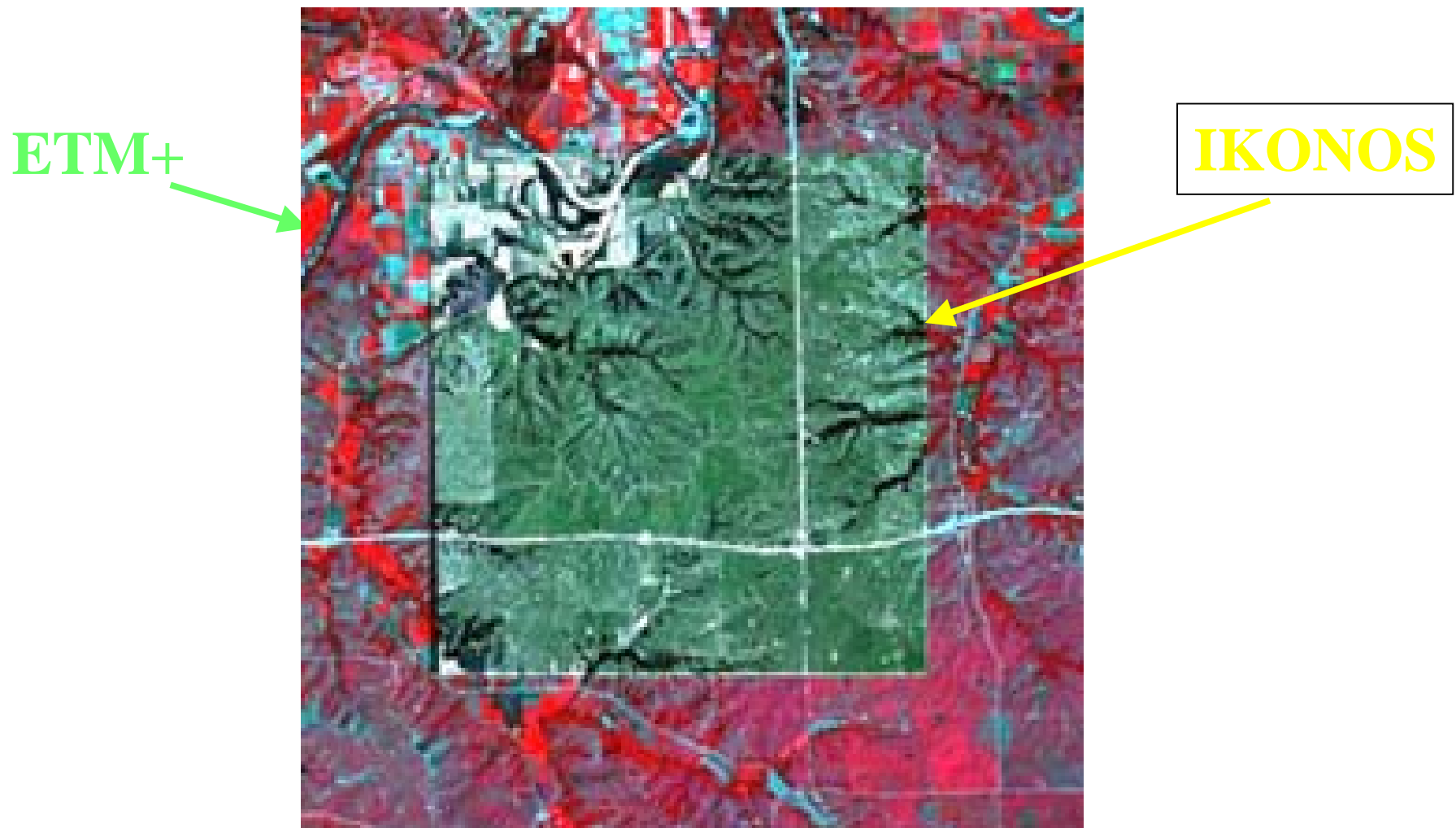
EOS Validation Core Sites

- Landsat-7/IKONOS/MODIS/SeaWiFS
 - Red and NIR for each sensor
 - 4 Spatial Resolutions:
 - IKONOS: 4 m; ETM+: 30 m; MODIS: 500m; SeaWiFS: 1000m
- 4 different sites:
 - **Coastal Area:** VA, Coast Reserve Area, October 2001
 - **Agriculture Area:** Konza Prairie in State of Kansas, July to August 2001
 - **Mountainous Area:** Cascades Site, September 2000
 - **Urban Area:** USDA Site, Greenbelt, MD, May 2001

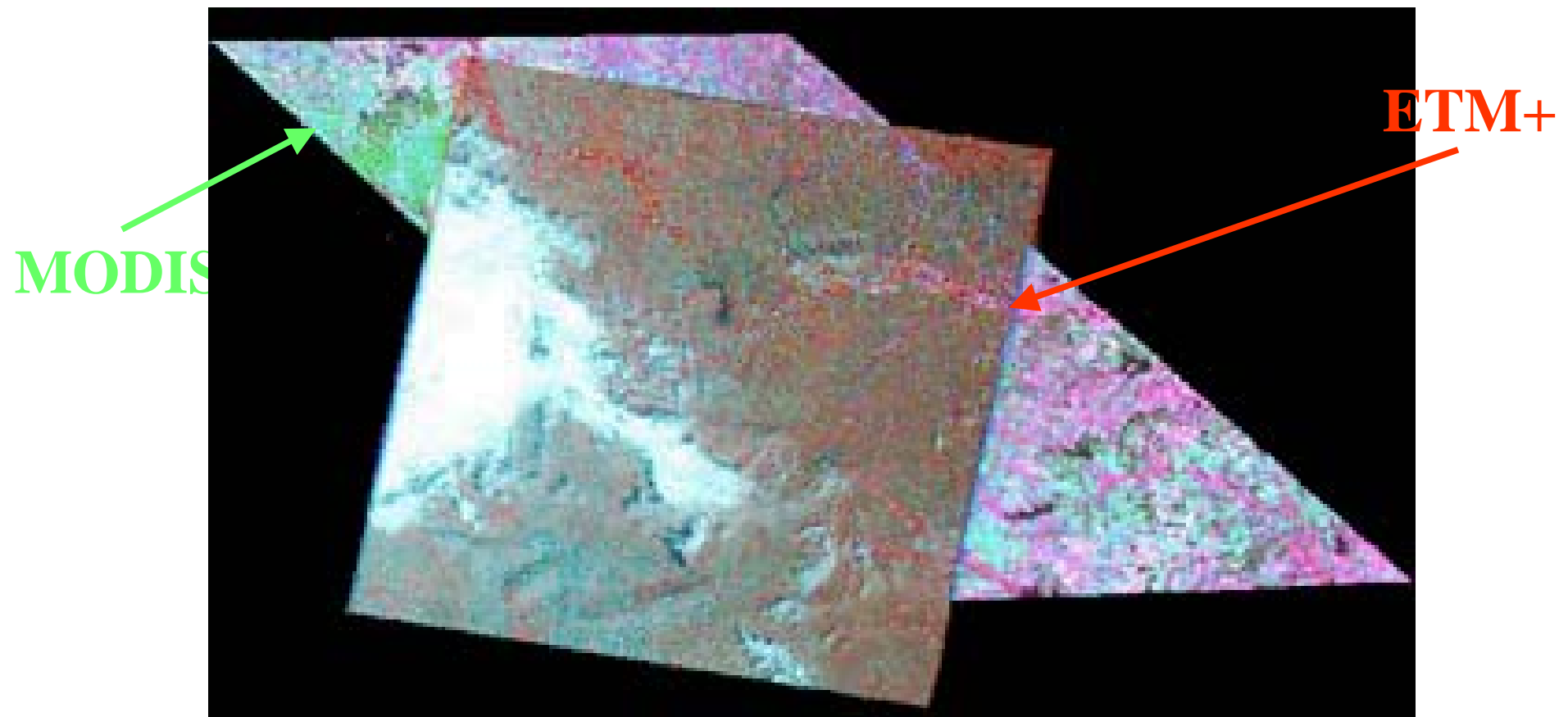
Test Data
EOS Validation Core Sites
ETM/IKONOS Mosaic of Coastal VA Data



Test Data
EOS Validation Core Sites
ETM/IKONOS Agricultural Konza Data



Test Data
EOS Validation Core Sites
ETM/MODIS of Agricultural Konza Data



Consistency Studies

IKONOS/ETM



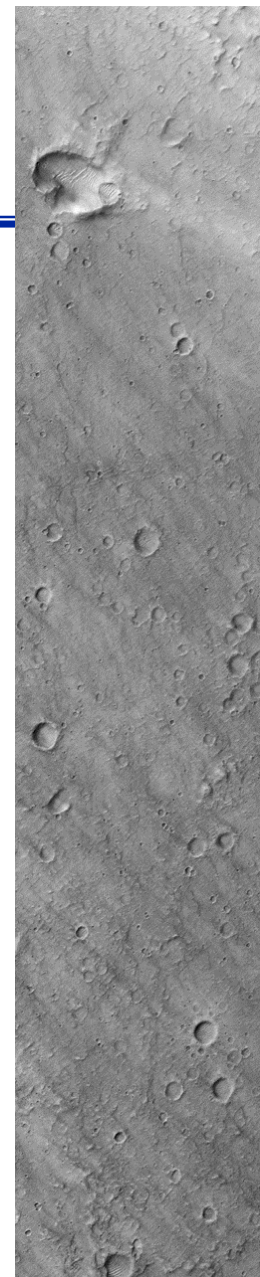
pairwise consistency

scale inconsistency

trgle/quad consistency

Mars Data

- 2 Pairs tested
- Image Sizes:
 - 2192x816
 - 3616x1024



Preliminary Results Mars Data



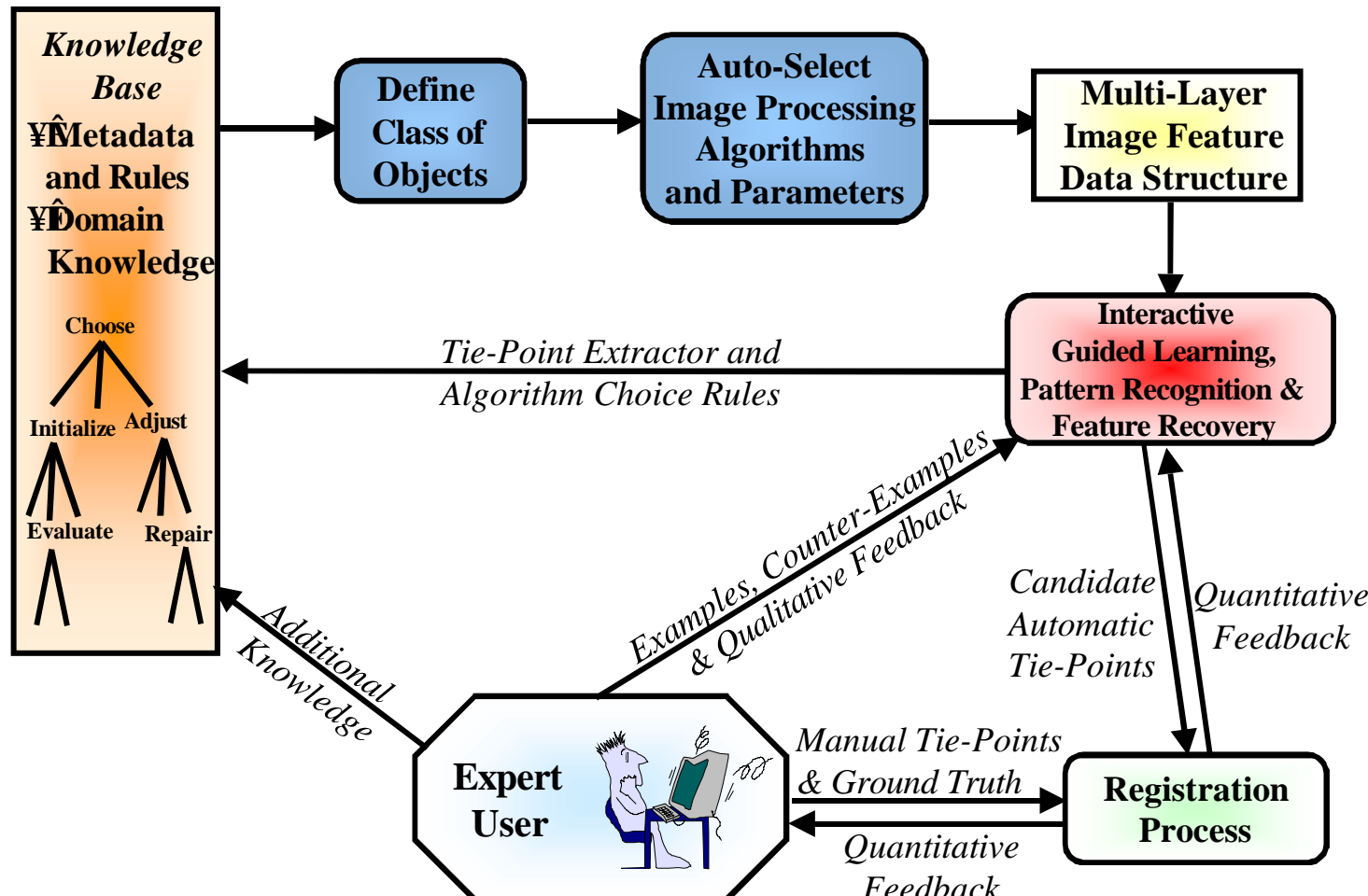
- Collaboration: Goddard Visualization Studio and ARC (Glenn Deardoff)
- Preliminary Results Using Small Chips and Normalized Correlation (using Fast Fourier Methods):
 - Chip Size: 128x128
 - Very Large Rotations, small rotations, small scale changes
 - Mean-Square Errors on the order of 1.1 pixels for one pair but 7.8 pixels for the other pair
- More work needed ...

Future Work - *Modular Framework*



- Systematic Modular Comparison
- Larger Number of Components
- Additional Datasets with Accurate Ground Truth
- Study:
 - Sensitivity to Initial Conditions
 - Computational and Memory Requirements
 - HP and Reconfigurable Implementations

Future Work - Automatic Extraction of Chips/Windows or Tie-Points Through Interactive Learning



Publications (1)



- **Journals**

- J. Le Moigne, W.J. Campbell, and R.F. Croomp, 2002, “An Automated Parallel Image Registration Technique of Multiple Source Remote Sensing Data,” IEEE Transactions on Geoscience and Remote Sensing, Vol. 40, No. 8, pp. 1849-1864, August 2002.
- S. Kaewpijit, J. Le Moigne, and T. El-Ghazawi, 2003, “Automatic Reduction of Hyperspectral Imagery Using Wavelet Spectral Analysis,” IEEE Transactions on Geoscience and Remote Sensing, Vol.41, No.4, pp.863-871, April 2003.
- W.J. Campbell, S. Chettri, P. Coronado, J.E. Dorband, J. Palencia, Y. Ranawake, J. Le Moigne, R.G. Lyon, G. Shirah, J.C. Tilton, “Hyperspectral Imaging Mining, UAV's, Direct Satellite Broadcast, Data Fusion, Computational optics, Scientific Visualizatiions and More,” Online Journal of Space Communication, Spring Issue No. 3, <http://satjournal.tcom.ohiou.edu/Issue03/applications.html>. Guest Editor: H.L. Bloemer.
- A. Cole-Rhodes, K. Johnson, J. Le Moigne, and I. Zavorin, 2003, “Multiresolution Registration of Remote Sensing Imagery by Optimization of Mutual Information Using a Stochastic

Publications (2)



-
- T. El-Ghazawi and J. Le Moigne, 2004, “Performance of the Wavelet Decomposition on Massively Parallel Architectures,” to be published in the International Journal of Computers and their Applications (IJCA).
 - S. Kaewpijit, J. Le Moigne, and T. El-Ghazawi, 2004, “Feature Reduction of Hyperspectral Imagery Using Wavelet-Based Principal Component Analysis,” to be published in Optical Engineering.
 - J. Le Moigne, N. Netanyahu, and J. Masek, 2004, “Geo-Registration of Landsat Data by Robust Matching of Wavelet Features,” to be published in IEEE Transactions on Geoscience and Remote Sensing.
 - T. El-Ghazawi, S. Kaewpijit, and J. Le Moigne, 2004, “Adaptive Reduction of Hyperspectral Data on Parallel Computers,” submitted to IEEE Transactions on Pattern Analysis and Machine Intelligence, June 2002.
 - I. Zavorin, and J. Le Moigne, 2004, “On the Use of Wavelets for Image Registration,” provisionnally accepted for IEEE Transactions on Image Processing, October 2003.
 - **J. Le Moigne A. Cole-Rhodes R. Eastman K. Johnson T. Jacqueline Le Moigne, 27**



Publications (3)

- **Conferences**

- T. El-Ghazawi, S. Kaewpijit, and J. Le Moigne, 2001, "Parallel Adaptive Reduction of Hyperspectral Data to its Intrinsic Dimensionality," Third IEEE International Conference on Cluster Computing, Cluster Computing '2001, Newport Beach, California, October 8-11, 2001.
- S. Kaewpijit, J. Le Moigne and T. El-Ghazawi, 2002, "Hyperspectral Imagery Dimension Reduction Using Principal Component Analysis on the HIVE," Science Data Processing Workshop, SDP'2002, Greenbelt, January 2002.
- J. Le Moigne, A. Cole-Rhodes, R. Eastman, K. Johnson, J. Morissette, N. Netanyahu, H. Stone and I. Zavorin, 2002, "Multi-Sensor Image Registration for On-the-Ground or On-Board Science Data Procesisng," Science Data Processing Workshop, SDP'2002, Greenbelt, January 2002, pps 9b1-9b6.
- S. Kaewpijit, J. Le Moigne and T. El-Ghazawi, 2002, "Spectral Data Reduction Via Wavelet Decomposition," SPIE Aerosense 2002, Wavelet Applications IX, Orlando, FL, April 2002.
- Cole-Rhodes, K. Johnson and J. Le Moigne, 2002, "Multi-Resolution Registration of Remote Sensing Images Using



Publications (4)

- S. Kaewpijit, J. Le Moigne and T. El-Ghazawi, 2002, “A Wavelet-Based PCA Reduction for Hyperspectral Imagery,” 2002 IEEE International Geoscience and Remote Sensing Symposium, IGARSS'02, Toronto, Canada, June 24-28, 2002.
- Zavorin, H. Stone and J. Le Moigne, 2002, “Iterative Pyramid-Based Approach to Subpixel Registration of Multisensor Satellite Imagery,” SPIE International Symposium on Optical Science and Technology 2002, Earth Observing Systems VII, Seattle, WA, July 7-11, 2002.
- J. Le Moigne, A. Cole-Rhodes, R. Eastman, T. El-Ghazawi, K. Johnson, S. Kaewpijit, N. Laporte, J. Morissette, N. Netanyahu, H. Stone and I. Zavorin, 2002, “Multiple Sensor Image Registration, Image Fusion and Dimension Reduction of Earth Science Imagery,” Invited Talk at the Fifth International Conference on Information Fusion, FUSION'2002, Annapolis, Maryland, July 8-11, 2002, pps 999-1006.
- Zavorin H. Stone and J. Le Moigne, 2003, “Evaluating Performance of Automatic Techniques for Sub-Pixel Registration of Remotely Sensed Imagery,” SPIE Electronic Imaging 2003, Image Processing: Algorithms and Systems II Conference, Santa Clara January 2003

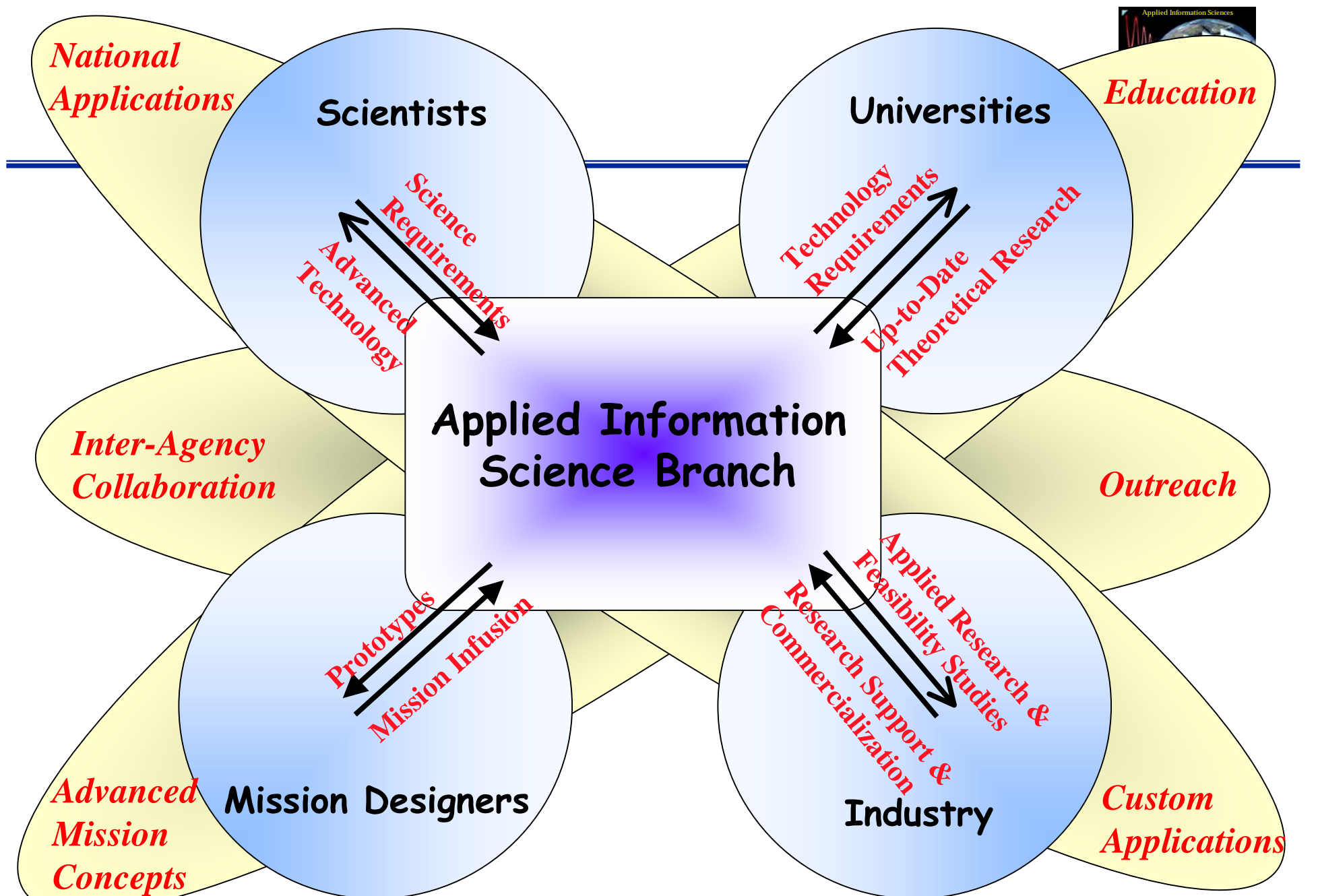


Publications (5)

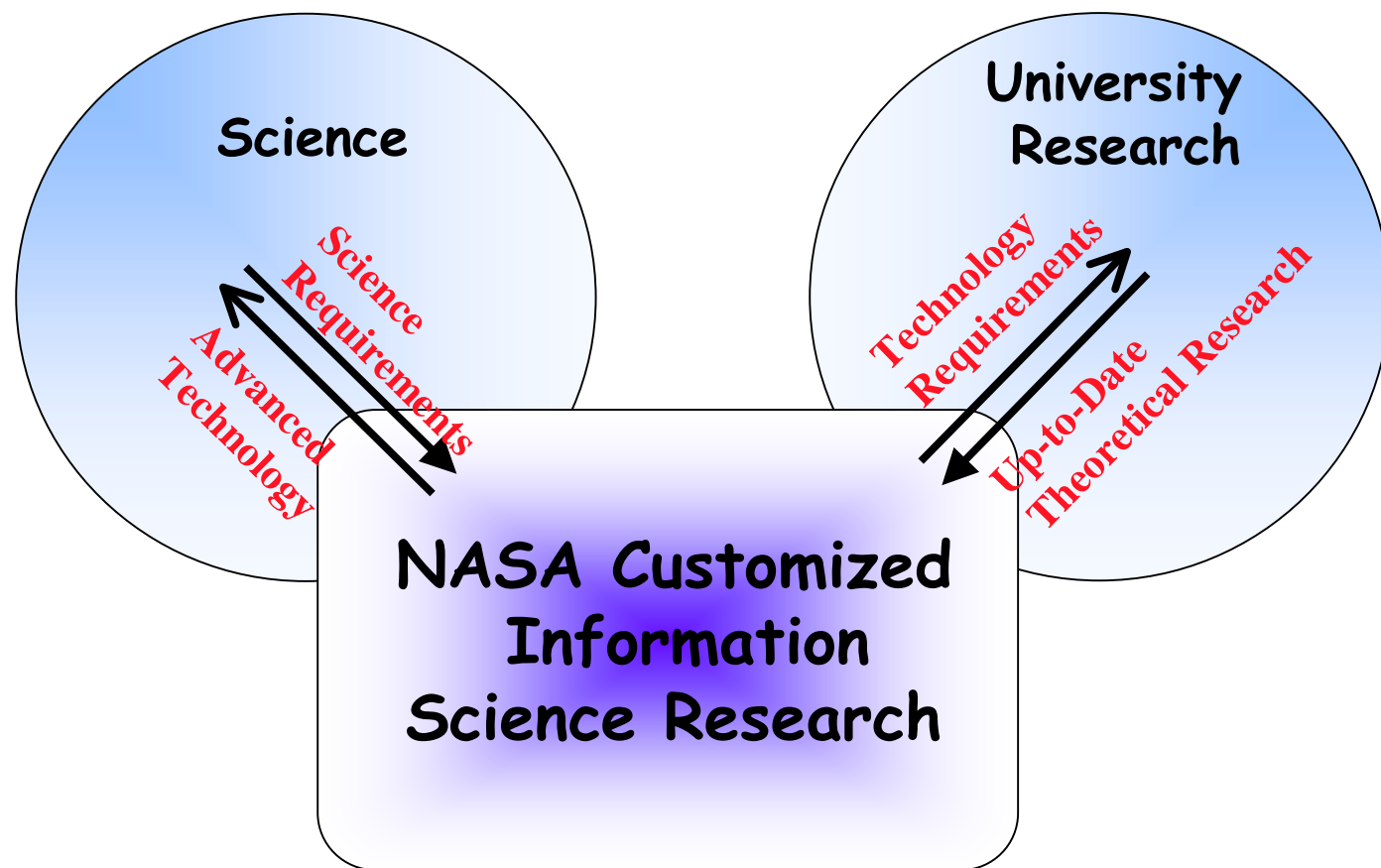
-
- S. Kaewpijit, J. Le Moigne and T. El-Ghazawi, 2002, “A Wavelet-Based PCA Reduction for Hyperspectral Imagery,” 2002 IEEE International Geoscience and Remote Sensing Symposium, IGARSS'02, Toronto, Canada, June 24-28, 2002.
 - Zavorin, H. Stone and J. Le Moigne, 2002, “Iterative Pyramid-Based Approach to Subpixel Registration of Multisensor Satellite Imagery,” SPIE International Symposium on Optical Science and Technology 2002, Earth Observing Systems VII, Seattle, WA, July 7-11, 2002.
 - J. Le Moigne, A. Cole-Rhodes, R. Eastman, T. El-Ghazawi, K. Johnson, S. Kaewpijit, N. Laporte, J. Morissette, N. Netanyahu, H. Stone and I. Zavorin, 2002, “Multiple Sensor Image Registration, Image Fusion and Dimension Reduction of Earth Science Imagery,” Invited Talk at FUSION'2002, Annapolis, Maryland, July 8-11, 2002.
 - Zavorin H. Stone and J. Le Moigne, 2003, “Evaluating Performance of Automatic Techniques for Sub-Pixel Registration of Remotely Sensed Imagery,” SPIE Electronic Imaging 2003, Image Processing: Algorithms and Systems II Conference, Santa



BACKUP SLIDES



Intelligent Data Understanding Context



Similarity Metrics

- Correlation

$$C(A, B) = \frac{\sum_i (a_i - \text{MeanA}) * (b_i - \text{MeanB})}{\sqrt{\sum_i (a_i - \text{MeanA})^2} * \sqrt{\sum_i (b_i - \text{MeanB})^2}}$$

- L2 Norm

$$E(p) = \sum (f - Q_p(g))^2$$

- Mutual Information:

$$I(A, B) = \sum_{a, b} h_{AB}(a, b) \cdot \log \frac{N \cdot h_{AB}(a, b)}{h_A(a) \cdot h_B(b)}$$

- Partial Hausdorff Distance:

$$H_k(A, B) = K^{\text{th}} \min_{a \in A} \min_{b \in B} \text{dist}(a, b)$$

($1 \leq k \leq |A|$; K^{th} is the k^{th} smallest element of set; $\text{dist}(a, b)$: Euclidean distance)



Matching Strategies

- Exhaustive Search
- Fourier Transform
 - Translations
 - Very Fast Implementations
- Gradient Descent
$$\begin{bmatrix} \sum f_x^2 & \sum f_x f_y & \sum Rf_x \\ \sum f_x f_y & \sum f_y^2 & \sum Rf_y \\ \sum Rf_x & \sum Rf_y & \sum R^2 \end{bmatrix} \begin{bmatrix} \Delta x \\ \Delta y \\ \Delta \theta \end{bmatrix} = \begin{bmatrix} \sum (f - g) f_x \\ \sum (f - g) f_y \\ \sum (f - g) R \end{bmatrix}$$
- Robust Feature Matching
 - Hierarchical Subdivisions of Search Space
 - Pruning of Search Space

Results Synthetic Test Data (1)

Synthetic Data wrt r256	Fast Correl	Gauss/L2/GD	Spline/L2/TRU	SimL/L2/TRU	SimB/L2/TRU	SimB/MI/Spall
r256						
Scale	1.0000	-	1.0000	1.0000	1.0000	1.0001
Rotation	0.0000	-	0.0000	0.0000	0.0000	0.0122
Shift-x	0.0000	-	0.0000	0.0000	0.0000	-0.0098
Shift-y	0.0000	-	0.0000	0.0000	0.0000	-0.0108
k_ratio	1.0000	-	1.0000	1.0000	1.0000	1.0001
thetaErr	0.0000	-	0.0000	0.0000	0.0000	0.0122
txErr	0.0000	-	0.0000	0.0000	0.0000	-0.0098
tyErr	0.0000	-	0.0000	0.0000	0.0000	-0.0108
Global Error	0.0000	-	0.0000	0.0000	0.0000	0.0145
i256_r2						
Scale	0.9998	0.9996	0.0000	0.9999	0.9999	1.0001
Rotation	1.9922	2.0132	2.0001	1.9977	1.9977	2.0082
Shift-x	-0.0723	-0.0186	0.0007	-0.0002	-0.0002	-0.0070
Shift-y	0.0662	0.0817	0.0005	-0.0012	-0.0001	0.0278
k_ratio	0.9998	0.9996	0.0000	0.9999	0.9999	1.0001
thetaErr	-0.0078	0.0132	0.0001	-0.0023	-0.0023	0.0082
txErr	-0.0723	-0.0186	0.0007	-0.0002	-0.0002	-0.0070
tyErr	0.0662	0.0817	0.0005	-0.0012	-0.0001	0.0278
Global Error	0.0980	0.0838	0.4061	0.0012	0.0002	0.0287
i256_tx1.3_ty3.7						
scale	0.9997	1.0000	1.0000	1.0000	0.9994	1.0000
Rotation	-0.0294	0.0047	-0.0003	-0.0006	-0.0019	0.0011
Shift-x	1.0131	1.2631	1.3001	1.2996	1.2953	1.2908
Shift-y	3.9321	3.4310	3.6983	3.6996	3.6955	3.7071
k_ratio	0.9997	1.0000	1.0000	1.0000	0.9994	1.0000
thetaErr	-0.0294	0.0047	-0.0003	-0.0006	-0.0019	0.0011
txErr	-0.1772	-0.0542	0.0012	0.0018	0.0033	-0.0132
tyErr	0.1966	-0.2630	-0.0021	-0.0011	-0.0046	0.0085
Global Error	0.2647	0.2685	0.0024	0.0021	0.0056	0.0157
i256_scl1.1						
Scale	1.0996	1.0878	1.1000	1.1000	1.0999	1.0999
Rotation	-0.0001	-0.0047	0.0002	-0.0003	0.0000	0.0049
Shift-x	0.0002	-0.0817	0.0004	0.0001	-0.0011	-0.0117
Shift-y	0.0005	0.0551	-0.0001	-0.0001	0.0043	0.0112
k_ratio	0.9996	0.9889	1.0000	1.0000	0.9999	0.9999
thetaErr	-0.0001	-0.0047	0.0002	-0.0003	0.0000	0.0049
txErr	0.0002	-0.0817	0.0004	0.0001	-0.0011	-0.0117
tyErr	0.0005	0.0551	-0.0001	-0.0001	0.0043	0.0112
Global Error	0.0005	0.0991	0.0004	0.0002	0.0045	0.0162

Results Synthetic Test Data (2)

i256_sc0.9						
Scale	0.9014	0.8893	0.9000	0.9000	0.9001	0.9001
Rotation	-0.0392	-0.0056	0.0000	0.0000	0.0005	0.0080
Shift-x	0.0000	0.1376	-0.0002	0.0003	0.0002	-0.0099
Shift-y	-0.0003	0.1059	-0.0005	-0.0013	-0.0022	-0.0251
k_ratio	1.0016	0.9881	1.0000	1.0000	1.0001	1.0001
thetaErr	-0.0392	-0.0056	0.0000	0.0000	0.0005	0.0080
txErr	0.0000	0.1376	-0.0002	0.0003	0.0002	-0.0099
tyErr	-0.0003	0.1059	-0.0005	-0.0013	-0.0022	-0.0251
Global Error	0.0003	0.1747	0.0006	0.0013	0.0022	0.0269
i256_r2_tx1.3_ty3.7						
Scale	1.0001	0.9999	1.0000	1.0000	1.0000	1.0000
Rotation	2.0131	1.9408	2.0002	2.0000	1.9992	2.0004
Shift-x	1.2172	1.1085	1.3001	1.3009	1.2981	1.3049
Shift-y	3.7748	3.6704	3.6997	3.7027	3.6950	3.7052
k_ratio	1.0001	0.9999	1.0000	1.0000	1.0000	1.0000
thetaErr	0.0131	-0.0592	0.0002	0.0000	-0.0009	0.0004
txErr	-0.1313	0.0297	-0.0008	0.0009	0.0013	0.0035
tyErr	0.0918	-0.0998	0.0000	0.0028	-0.0060	0.0057
Global Error	0.1602	0.1041	0.0008	0.0029	0.0061	0.0067
i256_sc0.9_r5_tx2.25						
Scale	0.9018	0.8897	0.9000	0.8999	0.9616	0.9000
Rotation	4.9566	5.0016	4.9996	4.9991	3.8120	5.0080
Shift-x	2.2876	2.5018	2.2505	2.2513	-4.3352	2.2517
Shift-y	0.3609	0.3697	-0.0014	-0.0026	4.7762	0.0034
k_ratio	1.0020	0.9885	1.0000	0.9999	1.0685	0.9999
thetaErr	-0.0434	0.0016	-0.0004	-0.0009	-1.1880	0.0080
txErr	0.0352	0.2777	0.0005	0.0015	-5.2331	0.0019
tyErr	0.2631	0.3732	-0.0024	-0.0047	2.5461	0.0214
Global Error	0.2652	0.4679	0.0024	0.0049	5.6300	0.0215
i256_sc1.1_r3_tx3.1_ty2.75						
Scale	1.1002	1.0890	1.1000	1.1000	1.0632	1.1000
Rotation	2.9922	2.8758	3.0001	3.0002	-3.0035	2.9981
Shift-x	2.7988	2.5993	3.1000	3.1002	-3.2838	3.0782
Shift-y	2.6428	2.6139	2.7500	2.7503	-8.8802	2.7507
k_ratio	1.0002	0.9900	1.0000	1.0000	0.9665	1.0000
thetaErr	-0.0078	-0.1242	0.0000	0.0002	-6.0035	-0.0019
txErr	-0.2802	-0.1089	-0.0002	-0.0003	-6.8974	-0.0166
tyErr	-0.1318	-0.4679	0.0001	0.0009	-10.6076	-0.0052
Global Error	0.3096	0.4828	0.0002	0.0010	12.8701	0.0174
MEAN ERROR	0.1569	0.2401	0.0590	0.0019	2.6456	0.0190

Results VA - IKONOS/ETM+

VA_Coast	Fast Correl	Gauss/L2/GD	Spline/L2/TRU	SimL/L2/TRU	SimB/L2/TRU	SimB/MI/Spall
IKONOS/Red-IKONOS/NIR						
Scale	1.0000	1.0001	1.0000	1.0000	0.9999	0.9997
Rotation	-0.0008	0.0117	-0.0005	-0.0002	0.0017	0.0271
Shift-x	0.0072	-0.2482	-0.1644	-0.2421	0.0523	0.7761
Shift-y	-0.0542	-0.3789	-0.4944	-0.5315	-0.5597	0.4016
IKONOS/Red-ETM/Red						
Scale	1.0661	1.0529	1.0662	1.0669	1.6094	1.0661
Rotation	0.0013	-1.5730	0.0204	0.0568	-1.3397	0.1040
Shift-x	12.8575	14.1783	12.9748	12.9902	-105.3350	13.0244
Shift-y	13.1722	15.8991	13.2198	13.3562	83.6175	14.1378
IKONOS/Red-ETM/NIR						
Scale	1.0619	1.0440	1.0515	3.0250	1.5185	1.0664
Rotation	-0.1210	-1.2434	1.5185	6.6137	7.5141	0.0103
Shift-x	12.3951	12.5628	10.6674	-205.4730	-45.6183	12.2158
Shift-y	12.2179	13.6363	9.3905	248.2180	69.9682	13.1563
IKONOS/NIR-ETM/Red						
Scale	1.0610	1.0524	1.0564	1.0516	0.9886	1.0674
Rotation	-0.9030	-2.0357	-1.0406	-1.1490	-0.5544	0.9718
Shift-x	10.3298	14.7560	27.7790	28.2731	-1.5585	16.0900
Shift-y	11.5491	17.9961	6.6591	6.5726	-1.7722	16.0972
IKONOS/NIR-ETM/NIR						
Scale	1.0654	1.0548	1.0651	1.0668	1.4050	1.0663
Rotation	-0.1093	-1.3526	0.0111	0.0375	3.7209	0.0063
Shift-x	12.5909	13.7730	13.0008	12.9493	-38.6769	12.8556
Shift-y	12.8984	14.5991	13.1058	13.2238	2.5245	13.2462
ETM/Red-ETM/NIR						
Scale	1.0000	0.9883	0.9998	0.9997	0.9998	1.0001
Rotation	0.0015	0.1146	-0.0146	-0.0214	-0.0136	-0.0020
Shift-x	-0.0670	-0.9907	-0.2048	-0.2243	-0.2107	0.8507
Shift-y	-0.0136	-1.2419	-0.4854	-0.6841	-0.5024	0.6654

Results - Konza IKONOS/ETM+

KONZA_Agriculture	Fast Correl	Gauss/L2/GD	Spline/L2/TRU	SimL/L2/TRU	SimB/L2/TRU	SimB/MI/Spall
IKONOS/Red-IKONOS/NIR						
Scale	No CV	1.0041	1.0467	1.0914	1.0193	0.9957
Rotation	No CV	0.2537	1.2699	3.1035	-0.0418	-0.0236
Shift-x	No CV	-0.0134	0.1735	14.5593	25.4888	-0.8333
Shift-y	No CV	-0.4962	22.0452	33.5204	1.8412	-1.6368
IKONOS/Red-ETM/Red						
Scale	1.0649	1.0084	1.0636	1.0658	0.9867	1.0640
Rotation	0.0721	-0.0202	0.0843	0.0765	-0.2897	0.0643
Shift-x	13.1959	5.9477	13.1744	13.0304	2.8568	13.2487
Shift-y	12.1727	6.8597	12.3728	12.3072	0.8004	12.2231
IKONOS/Red-ETM/NIR						
Scale	No CV	1.0154	1.0281	12.0354	0.9902	0.9504
Rotation	No CV	0.5424	0.7159	52.7968	0.0703	0.9943
Shift-x	No CV	-4.4192	-1.4182	1565.2800	-2.8466	6.9411
Shift-y	No CV	-3.2136	-4.2130	-683.6430	-4.5641	1.0748
IKONOS/NIR-ETM/Red						
Scale	No CV	1.0004	1.4113	7.1465	1.0379	0.6381
Rotation	No CV	0.0739	-11.5900	-13.2928	-0.5507	0.7490
Shift-x	No CV	-0.5760	-20.0565	216.9650	-1.3864	-8.1599
Shift-y	No CV	-1.0988	-50.7147	-691.9680	6.6042	-3.3631
IKONOS/NIR-ETM/NIR						
Scale	1.0649	1.0603	0.9978	1.0000	0.9473	1.0616
Rotation	0.0443	-0.0628	-0.0916	0.0000	0.2746	0.0020
Shift-x	13.1672	11.4400	0.1919	0.0000	-1.4771	13.4267
Shift-y	12.1068	12.1788	0.3016	0.0000	-4.1020	11.8736
ETM/Red-ETM/NIR						
Scale	1.0000	1.0009	0.9978	0.9986	1.0002	0.9999
Rotation	0.0000	0.0197	-0.0253	-0.0197	-0.1132	0.1153
Shift-x	0.0237	-0.3198	-1.4533	-1.5296	0.6607	0.7969
Shift-y	0.0105	-0.8417	1.3291	1.5235	0.9299	0.7991

Results - Cascades

IKONOS/ETM+



CASCADES_Mountains	Fast Correl	Gauss/L2/GD	Spline/L2/TRU	SimL/L2/TRU	SimB/L2/TRU	SimB/MI/Spall
IKONOS/Red-IKONOS/NIR						
Scale	1.0000	1.0005	1.0000	1.0000	1.0001	1.0003
Rotation	0.0003	0.0537	0.0006	0.0009	0.0009	0.0177
Shift-x	0.0135	-0.0091	-0.0240	-0.0464	-0.0362	0.0204
Shift-y	0.0135	0.0902	-0.1603	-0.2090	-0.1827	0.0535
IKONOS/Red-ETM/Red						
Scale	1.0644	1.0603	1.1006	1.0646	1.0642	1.0645
Rotation	0.0917	-0.1207	-0.0500	0.0703	0.0760	0.1302
Shift-x	8.6744	9.5412	11.4319	8.6323	8.6515	8.7768
Shift-y	10.1616	8.1125	12.3680	10.0836	10.0627	10.0392
IKONOS/Red-ETM/NIR						
Scale	1.0651	1.0604	0.9962	1.0000	1.0649	1.0640
Rotation	0.0883	-0.1026	-0.0316	0.0000	0.0878	0.1138
Shift-x	8.6944	9.5610	0.0321	0.0000	8.6573	8.8979
Shift-y	10.2174	8.1167	0.2538	0.0000	10.1193	10.2239
IKONOS/NIR-ETM/Red						
Scale	1.0641	1.0593	1.0765	1.0981	1.0646	1.0656
Rotation	0.0390	-0.1909	-0.5836	0.0694	0.0807	0.1277
Shift-x	8.5615	9.5090	10.5558	11.9510	8.5537	8.7318
Shift-y	10.1641	7.9072	9.9043	8.3562	10.1538	9.9239
IKONOS/NIR-ETM/NIR						
Scale	1.0647	1.0609	1.0649	1.0648	1.0649	1.0652
Rotation	0.1086	-0.0992	0.0725	0.0683	0.0714	0.1096
Shift-x	8.6681	9.5998	8.7279	8.6437	8.7094	8.6629
Shift-y	10.1669	8.1866	10.1404	10.1489	10.1394	10.1561
ETM/Red-ETM/NIR						
Scale	1.0000	1.0005	1.0000	1.0000	1.0001	1.0000
Rotation	-0.0006	0.0992	-0.0079	-0.0085	-0.0087	0.0929
Shift-x	0.0793	-0.0427	-0.1191	-0.0995	-0.1415	0.9420
Shift-y	-0.0290	0.1675	-0.1663	-0.1334	-0.2173	0.7340

Results - USDA IKONOS/ETM+

USDA_Urban	Fast Correl	Gauss/L2/GD	Spline/L2/TRU	SimL/L2/TRU	SimB/L2/TRU	SimB/MI/Spall
IKONOS/Red-IKONOS/NIR						
Scale	No CV	1.0443	1.0041	1.0637	0.9946	1.0003
Rotation	No CV	2.9476	-0.0587	-1.8167	0.0062	0.0810
Shift-x	No CV	-2.8000	-12.1204	-111.2490	-6.1957	0.7865
Shift-y	No CV	2.3448	-8.7683	-21.6973	-21.4048	0.8253
IKONOS/Red-ETM/Red						
Scale	1.0667	1.0184	5.0130	39.2684	0.9989	1.0729
Rotation	-0.0083	1.1602	-1.0558	-7.2146	0.1500	-0.1303
Shift-x	10.0562	3.1453	132.4880	1302.6200	2.7058	8.0719
Shift-y	14.2547	1.1701	49.5206	610.9530	0.7193	11.7209
IKONOS/Red-ETM/NIR						
Scale	No CV	0.9994	4.5364	92.7635	1.0047	0.0284
Rotation	No CV	0.2792	-1.9154	-13.9291	1.4735	-0.0556
Shift-x	No CV	-0.5906	30.2684	1245.8200	1.8242	-8.5007
Shift-y	No CV	-0.3171	89.4826	2233.2300	0.0525	-8.2559
IKONOS/NIR-ETM/Red						
Scale	No CV	1.0027	1.8762	1.0000	0.9820	0.0204
Rotation	No CV	0.0869	2.9724	0.0000	-0.0554	1.2481
Shift-x	No CV	-1.0203	-3.8586	0.0000	2.2506	-20.5221
Shift-y	No CV	0.0161	-13.2933	0.0000	0.4728	-9.4311
IKONOS/NIR-ETM/NIR						
Scale	1.0665	1.0624	2.3187	1.1610	0.9932	1.0682
Rotation	-0.0078	0.0316	-3.9027	-5.0480	1.4041	0.7500
Shift-x	10.0656	13.1350	69.8920	52.2085	2.0810	8.1570
Shift-y	14.2290	9.4498	-0.4875	-7.8668	0.0787	13.8792
ETM/Red-ETM/NIR						
Scale	No CV	1.0173	0.9979	0.9995	0.9992	1.0001
Rotation	No CV	4.0138	-0.0026	-0.0151	-0.0236	0.0026
Shift-x	No CV	-1.5203	1.1200	1.1777	-0.1887	0.3904
Shift-y	No CV	2.3550	-1.2877	0.4280	-2.5080	0.4810



Results - Konza ETM+/MODIS

KONZA ETM/MODIS	Fast Correl	Gauss/L2/GD	Spline/L2/TRU	SimL/L2/TRU	SimB/L2/TRU	SimB/MI/Spall
(1) MODIS_red_extract.img.raw/ ETM_red_r5760c7808.img_or99_l03.raw						
Scale	0.9614	0.9604	No CV	No CV	0.9596	0.9610
Rotation	0.0287	0.1582	No CV	No CV	-0.0129	0.1091
Shift-x	-10.1618	-10.3473	No CV	No CV	-10.1988	-10.5509
Shift-y	-6.9760	-7.3201	No CV	No CV	-7.2317	-7.3479
(2) MODIS_nir_extract.img.raw/ ETM_nir_r5760c7808.img_or99_l03.raw						
Scale	0.9696	1.0241	No CV	No CV	0.9598	0.9597
Rotation	0.0725	-0.2840	No CV	No CV	0.0137	-0.0574
Shift-x	-10.0550	-7.8410	No CV	No CV	-10.1789	-10.2096
Shift-y	-6.9060	-1.0741	No CV	No CV	-7.2523	-7.2092
(2) MODIS_red_extract.img.raw/ ETM_nir_r5760c7808.img_or99_l03.raw						
Scale	0.9900	0.9877	No CV	No CV	0.9602	0.9597
Rotation	-0.0051	1.4957	No CV	No CV	-0.0575	0.0011
Shift-x	0.8531	0.5930	No CV	No CV	0.2016	-10.3275
Shift-y	1.5344	-1.5227	No CV	No CV	-0.0105	-6.6447
(2) MODIS_nir_extract.img.raw/ ETM_red_r5760c7808.img_or99_l03.raw						
Scale	0.9892	1.0391	No CV	No CV	0.9675	0.0088
Rotation	0.5156	0.1314	No CV	No CV	-0.4004	1.7377
Shift-x	0.5650	-4.3975	No CV	No CV	4.2169	12.4947
Shift-y	0.7590	2.5483	No CV	No CV	0.2358	-3.9722
(2) MODIS_red_extract.img.raw/ MODIS_nir_extract.img.raw/						
Scale	0.9990	0.9836	1.0102	1.0006	1.0037	0.0246
Rotation	-0.0071	0.3087	-0.0538	-0.0949	-0.1998	-1.0004
Shift-x	0.4499	-3.4688	13.1378	3.4353	2.9486	-6.5125
Shift-y	0.2421	1.9552	-1.4173	0.7568	2.0034	-2.9157